Cardiovascular Diabetology

RESEARCH

Open Access

ALDH2 mediates the effects of sodium-glucose cotransporter 2 inhibitors (SGLT2i) on improving cardiac remodeling

Han Liu[1,2,3,4], Bingchen Jiang[1,2,3,4], Rui Hua[1,2,3,4], Xuehao Liu[1,2,3,4], Bao Qiao[1,2,3,4], Xiangxin Zhang[1,2,3,4], Xilong Liu[1,2,3,4], Wenjun Wang[5], Qiuhuan Yuan[1,2,3,4], Bailu Wang[6], Shujian Wei[1,2,3,4*] and Yuguo Chen[1,2,3,4*]

Abstract

Background Sodium-glucose cotransporter-2 inhibitors (SGLT2i) are now recommended for patients with heart failure, but the mechanisms that underlie the protective role of SGLT2i in cardiac remodeling remain unclear. Aldehyde dehydrogenase 2 (ALDH2) effectively prevents cardiac remodeling. Here, the key role of ALDH2 in the efficacy of SGLT2i on cardiac remodeling was studied.

Methods Analysis of multiple transcriptomic datasets and two-sample Mendelian randomization were performed to find out the differentially expressed genes between pathological cardiac hypertrophy models (patients) and controls. A pathological cardiac hypertrophy mouse model was established via transverse aortic constriction (TAC) or isoproterenol (ISO). Cardiomyocyte-specific ALDH2 knockout mice ($ALDH2^{CMKO}$) and littermate control mice ($ALDH2^{flox/flox}$) were generated to determine the critical role of ALDH2 in the preventive effects of dapagliflozin (DAPA) on cardiac remodeling. RNA sequencing, gene knockdown or overexpression, bisulfite sequencing PCR, and luciferase reporter assays were performed to explore the underlying molecular mechanisms involved.

Results Only ALDH2 was differentially expressed when the differentially expressed genes obtained via Mendelian analysis and the differentially expressed genes obtained from the multiple transcriptome datasets were combined. Mendelian analysis revealed that ALDH2 was negatively related to the severity of myocardial hypertrophy in patients. DAPA alleviated cardiac remodeling in mouse hearts subjected to TAC or ISO. ALDH2 expression was reduced, whereas ALDH2 expression was restored by DAPA in hypertrophic hearts. Cardiomyocyte specific ALDH2 knockout abolished the protective role of DAPA in preventing cardiac remodeling. ALDH2 expression and activity were increased in DAPA-treated neonatal rat primary cardiomyocytes (NRCMs), H9C2 cells and AC16 cells. Moreover, DAPA upregulated ALDH2 in peripheral blood mononuclear cells (PBMCs) from patients with type 2 diabetes. Sodium/proton exchanger 1 (NHE1) inhibition contributed to the regulation of ALDH2 by DAPA. DAPA suppressed the production of reactive oxygen species (ROS), downregulated DNA methyltransferase 1 (DNMT1) and subsequently reduced the ALDH2 promoter methylation level. Further studies revealed that DAPA enhanced the binding of nuclear

*Correspondence:
Shujian Wei
weishujian@sdu.edu.cn
Yuguo Chen
chen919085@sdu.edu.cn

Full list of author information is available at the end of the article

transcription factor Y, subunit A (NFYA) to the promoter region of ALDH2, which was due to the decreased promoter methylation level of ALDH2.

Conclusions The upregulation of ALDH2 plays a critical role in the protection of DAPA against cardiac remodeling. DAPA enhances the binding of NFYA to the ALDH2 promoter by reducing the ALDH2 promoter methylation level through NHE1/ROS/DNMT1 pathway.

Graphical abstract

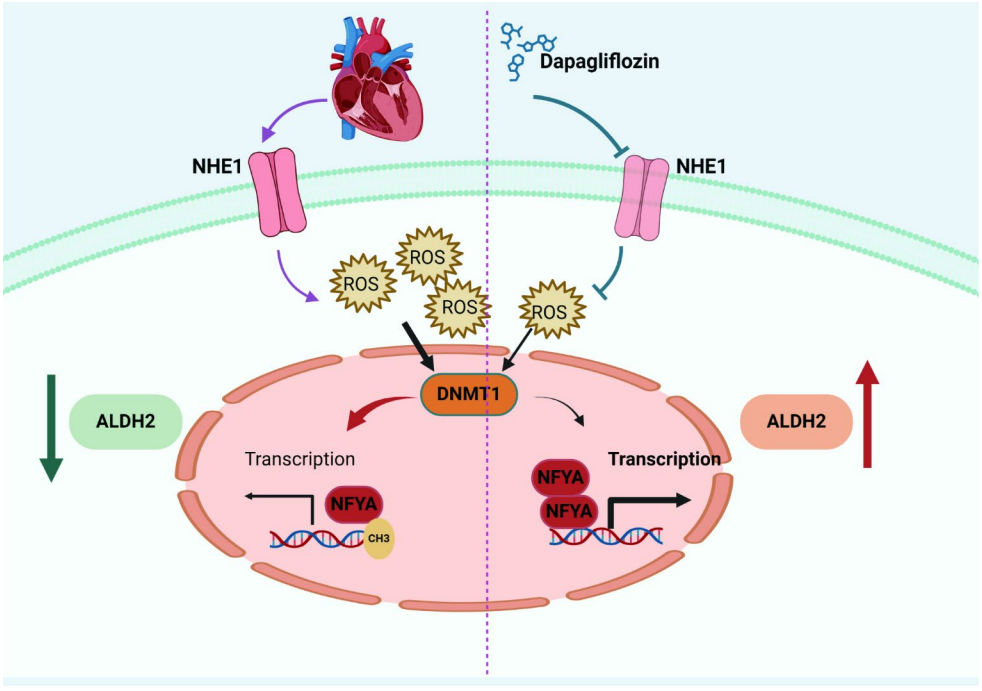

Keywords Cardiac remodeling, Sodium-glucose cotransporter-2 inhibitors, Aldehyde dehydrogenase 2, Sodium/proton exchanger 1, Methylation

Introduction

Heart failure is one of the leading causes of mortality worldwide [1]. As myocardial remodeling is the basic pathophysiological mechanism of heart failure, preventing or reversing myocardial remodeling is the key therapeutic target for heart failure [2, 3]. Myocardial remodeling is defined as structural and functional cardiac abnormalities, including a decrease in the number of cardiomyocytes, loss-of-function in cardiomyocytes, collagen deposition and scar formation, and dilation of the ventricular chamber in response to ischemia, pressure or volume overload, metabolic abnormalities, genetic mutations and some infectious or toxic stimuli [4, 5]. Although etiological correction and neurohumoral regulation are still the basis for HF treatment, preventing or reversing myocardial remodeling, such as beta-blockers, angiotensin-converting enzyme inhibitors, mineralocorticoid receptor antagonists, and sodium-glucose cotransporter 2 inhibitors (SGLT2i), has gradually become the key strategy for the treatment of HF [4, 6].

SGLT2i are glucose-lowering drugs that act on SGLT-2 proteins expressed in the proximal convoluted tubules [7]. They exert their effects by preventing the reabsorption of filtered glucose from the tubular lumen [7]. SGLT2i are recommended for both HF with a reduced ejection fraction and HF with a preserved ejection fraction [8]. Previous studies have revealed that SGLT2i improve cardiac remodeling through several molecular mechanisms including suppressing the inflammatory response, preventing cardiac fibrosis, reducing cell apoptosis, and improving mitochondrial function [9, 10]. SGLT2i can ameliorate adverse cardiac remodeling and heart failure by enhancing myocardial energetics [11] and exerting effects on iron availability and utilization [12, 13]. However, the cardiovascular protective effect of SGLT2i remains to be further explored because of the absence of SGLT2 on the surface of cardiomyocytes [14].

Aldehyde dehydrogenase 2 (ALDH2) is a mitochondrial enzyme that plays a key role in the detoxification of toxic aldehydes such as 4-hydroxynonenal (4-HNE)

and acetaldehyde [15]. In the recent decades, the role of ALDH2 in cardiovascular diseases, including cardiac remodeling, has been extensively explored [16]. ALDH2 can improve cardiac remodeling through several mechanisms including enhancing mitophagy, regulating angiogenesis, preventing fibrosis and cell death, and reducing the production of reactive oxygen species (ROS) and toxic aldehydes [16, 17]. Recently, it was reported that empagliflozin ameliorates ALDH2 gene mutation-induced endothelial cell dysfunction, but whether SGLT2i affects ALDH2 activity and expression has never been studied [18]. Here, we focused on exploring the key role of ALDH2 in the protective effect of SGLT2i on cardiac remodeling and elucidating the underlying mechanisms by which SGLT2i regulate ALDH2.

Materials and methods

Human subjects

Newly diagnosed patients with type 2 diabetes took dapagliflozin (DAPA, 10 mg/d) orally for three days. Ficoll density gradient separation (17144002, Cytiva) and red cell lysis solution (BL503B, Biosharp) were used to isolate human peripheral blood mononuclear cells (PBMCs) according to the manufacturers' protocols. This study was approved by the Ethics Committee of Qilu Hospital of Shangdong University, and all patients provided written informed consent.

Mendelian randomization

We used two-sample MR (Mendelian Randomization) to estimate the causal effect of plasma protein onpathological cardiac hypertrophy. The plasma protein data were derived from 4,907 plasma proteins detected in 35,559 Icelanders. The summary statistics of pathological cardiac hypertrophy were obtained from the FinnGen consortium R7 release data (3100 cases and 156711 controls). Inverse variance weighted, MR-Egger, weighted median and weighted models were used to examine the causal associations between plasma protein levels andpathological cardiac hypertrophy.

RNA-sequencing (RNA-seq) analysis

All public transcriptome data were obtained from the GEO public database. Bioinformatics analysis of the RNA-seq was performed at https://www.omicstudio.cn/tool and http://www.sangerbox.com/. RNA sequencing of mouse heart tissues was performed on the Illumina sequencing platform (LC-BIO, Hangzhou, China).

Animals

All animal experiments and methods followed ethical guidelines for animal studies and were approved by the Institutional Animal Care and Use Committee of Qilu Hospital of Shandong University. Male and female (8-10-week-old) C57/6J mice were obtained from Beijing Vital River Laboratory Animal Technology (Beijing, China). $ALDH2^{flox/flox}$ mice on a C57/6J background and αMyHC-Cre mice were purchased from Cyagen Biosciences (Suzhou, China). Cardiomyocyte-specific ALDH2 knockout mice ($ALDH2^{flox/flox}$αMyHC-Cre, $ALDH2^{CMKO}$) and their littermates ($ALDH2^{flox/flox}$) were generated by breeding $ALDH2^{flox/flox}$ mice with αMyHC-Cre mice. The genotypes of the transgenic mice were detected by polymerase chain reaction (PCR) analysis via DNA from the mouse tail.

Transverse aortic constriction

The mice (body weight 25±2 g) were anesthetized with pentobarbital, intubated, and subjected to transsternal thoracotomy. The transverse aorta was constricted by tying a 7–0 nylon suture ligature against a 26-gauge needle between the innominate and left carotid arteries. The sham operation was the same as that described above, except that the knot was not tied.

Subcutaneous injection of isoproterenol

C57BL/6J male mice were injected with isoproterenol (ISO, 5 mg/kg/d, I5627, Sigma) for 2 weeks as previously described [19].

Dapagliflozin treatment

The mice were treated with DAPA (1 mg/kg/d, S1548, Selleck) through intragastric administration after TAC or ISO injection [20].

Western blot analysis

The extracted proteins were prepared by lysing tissues or cells in RIPA lysis buffer, separated by sodium dodecyl sulfate–polyacrylamide gel electrophoresis (SDS–PAGE), and then transferred onto 0.45 μm polyvinylidene difluoride (PVDF) membranes (Merck Millipore, Billerica, MA). The membranes were incubated at 4 °C overnight with primary antibodies. The details of the primary antibodies used are shown in Supplementary Table 1. After washing, the membranes were incubated with the corresponding horseradish peroxidase–coupled secondary antibodies. The quantification of the bands was performed using ImageJ software (version 1.53c, NIH).

RNA isolation and quantitative real-time-PCR (qRT-PCR)

Total RNA was extracted from cardiomyocytes and heart tissue using TRIzol reagent (15596018, Thermo Fisher). The RNA samples (1ng) were reversely transcribed to cDNA via the Hiscript®III Reverse Transcriptase Kit (R223-01, Vazyme). qRT-PCR analysis was performed on a QuantStudio 5 Real-Time PCR Detection System using ChamQ Universal SYBR qPCR Master Mix (Q711-02, Vazyme) with specific primers. The relative expression

levels of each gene were quantified using the 2−ΔΔCT method and normalized to the amount of endogenous glyceraldehyde-3-phosphate dehydrogenase (GAPDH). The sequences of the specific primers used for qRT-PCR in this study are listed in Supplementary Table 1.

Histological staining

The mice were euthanized and heart sections (5 μm intervals) were stained with Masson (G1340, Solarbio) and Sirius red (G1472, Solarbio) according to routine procedures. Heart sections were incubated with wheat germ agglutinin-Alexa488 (29022-1, Biotium) at 4℃ overnight to visualize the membranes and with 4,6-diamidino-2-phenylindole (DAPI) to observe the nucleus. All images were visualized with an automated fluorescence microscope (Olympus SLIDEVIEW VS200).

Echocardiographic assessment

Echocardiography measurements were performed with a high-resolution microimaging system equipped with a 30-MHz transducer (Vevo2100, Visual Sonics) to evaluate the cardiac function of the mice. Cardiac echocardiography data were recorded on a heating plate at 37 °C. The mice were anesthetized via inhalation of 1.5–2% isoflurane, and the heart rate was maintained at 450–500 beats/min. M-mode cardiac images of the left ventricle (LV) from the left parasternal long-axis view at the papillary muscle level were used to assess the LV wall thickness and LV dimensions, including interventricular septal thickness at end systole (IVSs), LV posterior wall thickness at end diastole (LVPWd), LV posterior wall thickness at end systole (LVPWs), end-diastolic dimensions of the LV (LVEDd) and end-systolic dimensions of the LV (LVEDs).

Cells and culture conditions

Primary neonatal rat cardiomyocytes (NRCMs) were isolated from the ventricles of 2-day-old Sprague-Dawley rats (Cyagen Biosciences, Suzhou, China). After thoracotomy, the hearts were extracted from the body and transferred immediately into cold Hanks balanced salt solution. The tissue was cut into small pieces and transferred into a conical flask containing 0.04% collagenase type II (C6885, Sigma) to a 37 °C cell culture incubator with magnetic stirring (150 rpm) for 1 h. The fibroblasts were then removed using a differential attachment technique. NRCMs were seeded at a density of 6×10^5 cells per well onto gelatine-coated six-well culture plates in plating medium consisting of DMEM (Gibco) supplemented with 20% fetal calf serum (FBS), BrdU (0.1 mmol/L, to inhibit the proliferation of fibroblasts) and penicillin/streptomycin at 37 °C in 5% CO2. The H9C2 cell line (CL-0089) and AC16 cell line (CL-0790) were provided by Procell (Wuhan, China). The cells were cultured under permissive conditions (37 °C, 5% CO2) in DMEM (Gibco) containing 10% FBS.

The cells were then treated with 10μM ISO for 48 h to induce cardiomyocyte hypertrophy. DAPA, empagliflozin or N-acetylcysteine were used to treat cardiomyocytes according to experimental requirements.

Mitochondria extraction

After different treatments, the NRCMs were harvested, and the mitochondria were extracted using a cell mitochondria isolation kit (Beyotime, Haimen).

ALDH2 activity

ALDH2 activity was measured with a Mitochondrial Aldehyde Dehydrogenase (ALDH2) Activity Assay Kit (ab115348, Abcam).

Immunofluorescence staining

The samples were subsequently fixed with 4% paraformaldehyde for 15 min and permeabilized with 0.5% (v/v) Triton X-100 in PBS for 20 min at 37 °C. After washing, the samples were blocked in 5% (w/v) BSA in PBS for 40 min and incubated with primary antibody at 4 °C overnight. The primary antibodies used in our studies were shown in Supplementary Table 2. Images were captured with a confocal laser scanning microscope (Leica TCS SP8, Wetzlar, Germany). The positive areas were measured with ImageJ software (version 1.8.0). Data were expressed as a percentage of the total area positively stained.

Molecular docking and prediction

Molecular simulation of the binding of DAPA with NHE1 was performed via AutoDock version 4.2.6. PyMOL 2.5 software was then used to analyze the hydrogen bonds and bond lengths within the interactions. DAPA structure file source: https://pubchem.ncbi.nlm.nih.gov/; NHE1 (7dsw.A) structure file source: https://www.rcsb.org/.

Viral infection

Lentiviruses that overexpress NHE-1 were synthesized by Boshang (Jinan, China) and transfected into H9C2 cells according to the manufacturer's instructions. Stably transfected clones were isolated in medium containing puromycin (ant-pr-1, InvivoGen). Individual puromycin-resistant clones were subsequently selected.

BSP analysis of ALDH2

The methylation status of the ALDH2 promoter was determined via the BSP method. Genomic DNA was isolated with a DNeasy Blood & Tissue Kit (69504, Qiagen) and then subjected to bisulfite modification using the EZ DNA Methylation Kit (59104, Qiagen). The

bisulfite-treated genomic DNA was amplified via PCR using the Thermal Cycler from Applied Biosystems (Foster City, CA). The PCR products were electrophoretically separated and purified. The products were subsequently cloned and inserted into the pGEM-T easy vector for Sanger sequencing. Five clones were sequenced for each DNA sample. The percentage of methylation was calculated from the number of methylated CpGs divided by the total number of CpG loci. The primers used were designed with Methyl Primer Express 1.0 from Applied Biosystems. The primer sequences for ALDH2 were as follows: forward, 5′- TTGTAYGGATGGGATTTATAAG −3′; reverse, 5′- AAACTAAACRAAACTTAACAAAAC −3′.

Short interfering RNA transfection

Short interfering RNAs (siRNAs) targeting DNMT1 were purchased from Boshang (Jinan, China). NRCMs were seeded in 6-well plates, transfected with the corresponding short interfering RNA mixed with Lipofectamine™ RNAiMAX (13778075, Thermo Fisher) and cultured for 24 to 48 h. The cells were then treated with H2O2 or DAPA and harvested for the following experiments.

ROS measurement

The ROS levels in the cells were assessed with a Reactive Oxygen Species Assay Kit CA1410 (Solarbio, Beijing). ROS in heart tissues were detected with dihydroethidium solution (DHE, 5 μmol/L, Beyotime, S0063, Nanjing). Briefly, 5 μm cryosections of hearts were incubated with DHE in a light-protected humidified chamber at 37 °C for 30–40 min. An inverted fluorescence microscope was used to observe and obtain fluorescence micrographs. The levels of ROS in the heart tissues were further determined via an available ELISA kit (KYY-43700M2, Keyybio).

Luciferase reporter assay

Cardiomyocytes (H9C2) were seeded at 1×10^5 cells/well in 12-well plates and allowed to adhere overnight. Nfya-NC or nfya-flag and the pGL3-ALDH2 promoter were cotransfected into cells. Luciferase activities were determined via a dual-luciferase reporter assay system (DL101-01, Vazyme).

CUT-Tag

Concanavalin A coated magnetic beads were prepared according to Hyperactive Universal CUT&Tag Assay Kit (TD904, Vazyme) protocol. Activated beads were then added and incubated at room temperature for 10 min. Cardiomyocytes (H9C2) were sequentially incubated sequentially with ConA beads, primary antibodies (anti-DNMT1 antibody, anti-NFYA antibody), secondary antibody (Goat anti-Rabbit IgG H&L, AB206-01-AA, Vazyme) and Hyperactive PG-TN5/PA-TN5 Transposon, and then fragmented. Fragmented DNA was extracted from the samples and amplified by PCR.

Statistical analysis

All the analyses were performed using GraphPad Prism 8. The experimental data were reported as the mean ± SEM. For experiments with two groups, statistical comparisons were conducted using the two-tailed Student's t test. One-way ANOVA with Tukey's test was generally employed for multiple-group comparisons. Mendelian Randomization analysis was performed using R software. Statistical significance was defined as $P<0.05$.

Results

ALDH2 is decreased in pathological cardiac hypertrophy

Through the analysis of multiple transcriptomic datasets, we found that ALDH2 was downregulated in the hearts of several pathological cardiac hypertrophy models (Supplemental Fig. 1). The overlap of the multiple transcriptome datasets revealed that 88 genes were differentially expressed in the hearts of hypertrophic models and controls (Fig. 1A). Mendelian analysis revealed that 169 plasma proteins were differentially expressed in the hearts from patients with pathological cardiac hypertrophy compared with those in hearts from controls (Fig. 1B). When the differentially expressed genes obtained via Mendelian analysis and the differentially expressed genes obtained from the multiple transcriptome datasets were combined, only ALDH2 was differentially expressed (Fig. 1B). Further Mendelian analysis revealed that ALDH2 was negatively related to the severity of myocardial hypertrophy (Fig. 1C). Using a TAC model, we also found that ALDH2 was decreased in pressure overload - induced pathological cardiac hypertrophy(Fig. 1D and E).

DAPA upregulates ALDH2 in pressure overload- induced or isoproterenol-induced hypertrophic hearts

To determine the effects of SGLT2i on cardiac remodeling, DAPA was administered to male mice subjected to TAC surgery. DAPA was administered intraperitoneally at a dose of 1 mg/kg/d on Day 3 after TAC surgery (Supplementary Fig. 2A-2B). Mice in TAC group developed obviously hypertrophied hearts (Fig. 2A and B). Compared with that in the TAC group, cardiac hypertrophy was significantly alleviated by DAPA (Fig. 2A and B). Compared heart weight normalized by tibial length, DAPA still had a protective effect on TAC-induced cardiac hypertrophy (Fig. 2C). Staining of heart cross-sections also indicated that cardiomyocyte hypertrophy was alleviated by DAPA (Fig. 2D and E). Echocardiographic examinations revealed that LV hypertrophy was prevented (Fig. 2F and K) and cardiac function was

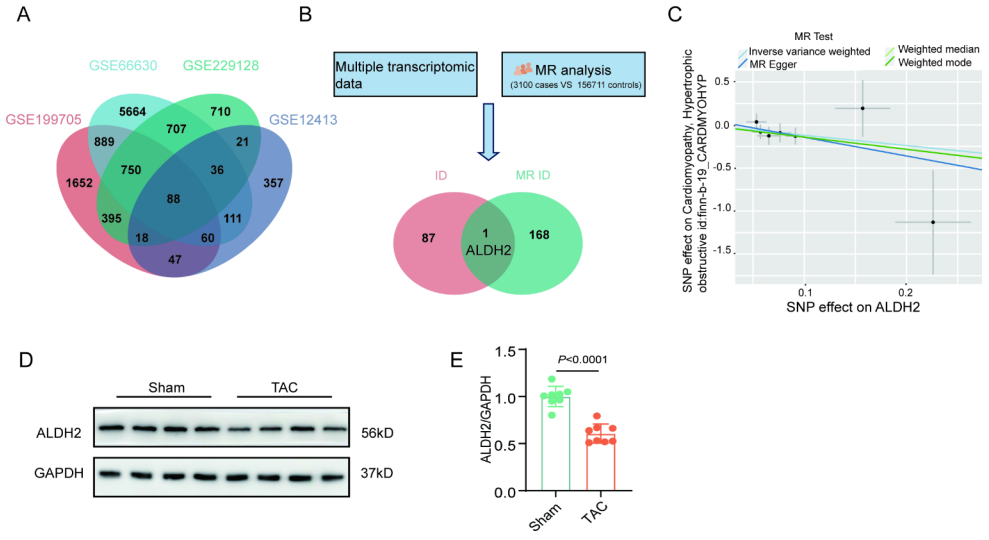

Fig. 1 ALDH2 is downregulated in myocardial remodeling. **A**, Venn diagram of the mRNA sequencing and reanalysis data of multiple transcriptomes. **B**, Overlaps of the results of the mRNA sequencing and Mendelian randomization study. **C**, Scatter plots illustrating the causal relationship between ALDH2 andpathological cardiac hypertrophy, as determined through a Mendelian randomization study. **D**-**E**, Western blot analysis of ALDH2 levels in the heart tissues of sham and TAC model mice ($n=8$). *P* values are indicated

preserved by DAPA (Fig. 2L and M). Moreover, the mice in the TAC group developed significant cardiac fibrosis, whereas DAPA markedly reduced the extent of cardiac fibrosis (Supplemental Fig. 2C-2 H). In female mice subjected to the TAC model, DAPA also prevented cardiac hypertrophy (Supplemental Fig. 3A-3 K). Similar to the changes in male mice, ALDH2 was decreased in hearts from female mice subjected to TAC surgery and this decrease was effectively reversed by DAPA (Supplemental Fig. 3L-3O). To further confirm the beneficial effects of DAPA in preventing cardiac remodeling, an ISO-induced cardiac hypertrophy model was used and consistent with the results from the TAC-model, DAPA had a preventive effect on ISO-induced cardiac hypertrophy (Supplemental Fig. 4).

RNA-sequencing analysis performed of DAPA-treated mouse heart tissues revealed that the mRNA expression of *ALDH2* was upregulated by DAPA in hearts subjected to TAC (Fig. 2N). Quantitative RT-PCR confirmed the upregulation of *ALDH2* by DAPA (Fig. 2O). Moreover, the protein expression of ALDH2 was also increased by DAPA in mouse hearts subjected to TAC (Fig. 2P).

ALDH2 deficiency eliminates the effects of DAPA on pressure overload - induced pathological cardiac hypertrophy

To elucidate the role of ALDH2 in the effect of DAPA on cardiac remodeling, ALDH2^{CMKO} mice were generated (Fig. 3A and B, Supplemental Fig. 5A-5 C). ALDH2^{CMKO} mice presented no abnormalities in the size of their hearts compared with control mice (Supplemental Fig. 5D-5E). In the TAC model, ALDH2 ^{CMKO} mice presented a significantly lower survival rate than control mice and this susceptibility of ALDH2^{CMKO} mice to TAC model could not be improved by DAPA (Fig. 3C). Cardiomyocyte-specific ALDH2 deficiency aggravated TAC-induced cardiac hypertrophy (Fig. 3D and O). Importantly, the protective effects of DAPA on pressure overload-induced pathological cardiac hypertrophy were abolished in ALDH2^{CMKO} mice (Fig. 3D and O). Moreover, cardiac fibrosis cannot be prevented by DAPA in ALDH2^{CMKO} mice (Supplemental Fig. 5F-5G).

DAPA increases ALDH2 expression and activity in cardiomyocytes

Similar to its effect on hearts in vivo, DAPA prevented the increase in the cell surface area and reduced the mRNA levels of the hypertrophic markers– ANP and BNP in iso-treated cardiomyocytes (Supplemental Fig. 6). Notably, DAPA increased the protein expression of ALDH2 in NRCMs (Fig. 4A and D). Similar results were found in H9C2 and AC16 cells (Fig. 4E and H). Moreover, we found DAPA upregulated ALDH2 in PBMCs from patients with type 2 diabetes (Fig. 4I and J). Further studies with empagliflozin indicated that it could also increase the protein expression of ALDH2 in NRCMs (Supplemental Fig. 7). In addition to the protein level, we also found that DAPA increased the enzymatic activity of ALDH2 (Fig. 4K), which may be due to the translocation of PKC-ε to mitochondria (Supplemental Fig. 8).

NHE1 mediates the regulation of ALDH2 by DAPA

Consistent with previous studies [14], we did not observe SGLT2 expression in cardiomyocytes (Supplementary Fig. 9). NHE1 is a common target of SGLT2 inhibitors in cardiomyocytes [14, 21]. DAPA could directly bind to

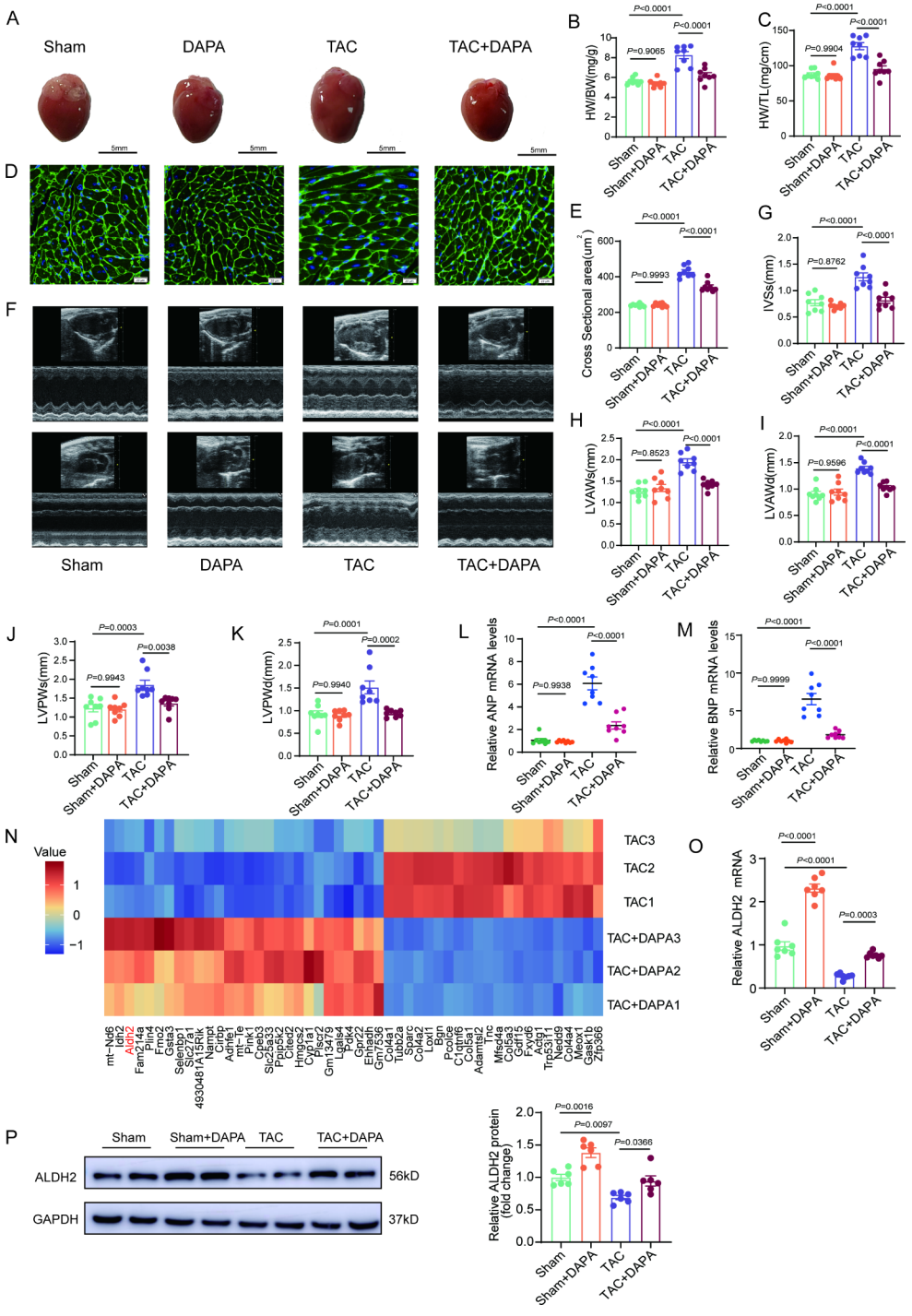

Fig. 2 DAPA increases ALDH2 expression in hypertrophic hearts. **A**, Representative macroscopic images of the indicated groups after treatment with TAC or DAPA (1 mg/kg/d). **B**-**C**, Ratios of heart weight/body weight (HW/BW) and heart weight/tibia length (HW/TL) in the four groups of mice ($n = 8$). **D**-**E**, Histological analysis of wheat germ agglutinin (WGA) staining in four groups of mice ($n = 8$, scale bar = 20 μm). **F**-**K**, Echocardiographic measurements of IVSs, LVAWs, LVAWd, LVPWs and LVPWd are shown ($n = 8$). **L**-**M**, Real-time quantitative PCR analysis of the *ANP* and *BNP* mRNA levels in the heart tissues of the four groups of mice ($n = 8$). **N**N, Heatmap differentially expressed genes in heart tissues after TAC or TAC + DAPA for 2 weeks. **O**, Real-time quantitative PCR analysis of *ALDH2* mRNA levels in heart tissues of the four groups of mice ($n = 7$). **P**, Western blot analysis of ALDH2 levels in heart tissues of the four groups ($n = 6$). *P* values are indicated

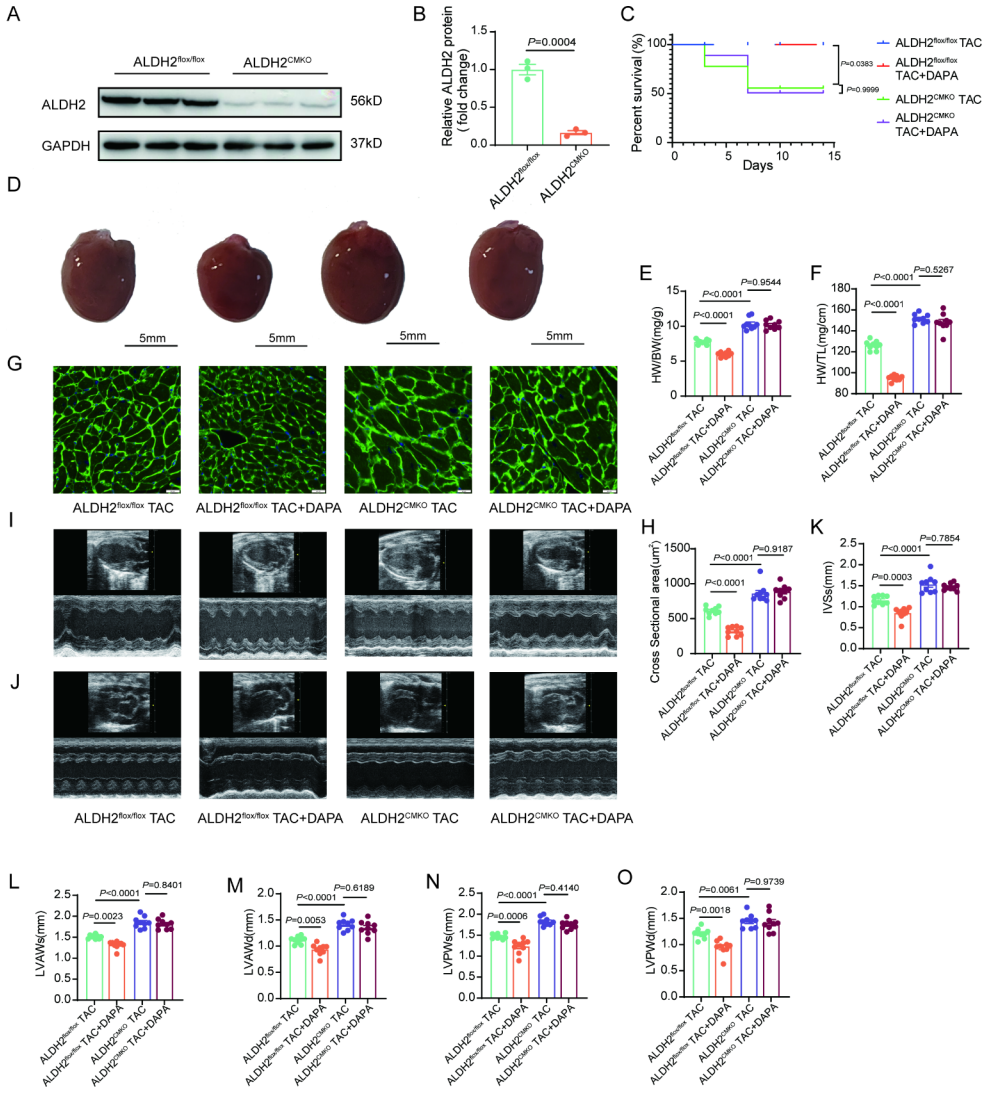

Fig. 3 Loss of ALDH2 abolishes the cardioprotective effects of DAPA in vivo. **A**-**B**, Western blot analysis of ALDH2 levels in heart tissues from ALDH2^{CMKO} mice and littermate controls ($n = 3$). **C**, Survival curves of the indicated groups. **D**, Representative macroscopic images of the indicated groups after TAC or DAPA (1 mg/kg/d) treatment for 2 weeks. **E**-**F**, Ratios of heart weight/body weight (HW/BW) and heart weight/tibia length (HW/TL) in the four groups of mice ($n = 9$). **G**-**H**, Histological analysis of wheat germ agglutinin (WGA) staining in four groups of mice ($n = 9$, scale bar = 20 μm). **I**-**O**, Echocardiographic measurements of IVSs, LVAWs, LVAWd, LVPWs and LVPWd are shown ($n = 9$). *P* values are indicated

the NHE1 receptor according to molecular docking and prediction (Fig. 5A). Using an NHE1 inhibitor, we found that NHE1 inhibition increased the expression of ALDH2 (Fig. 5B and C). NHE1 overexpression downregulated the expression of ALDH2 and attenuated the effect of DAPA on ALDH2 (Fig. 5D and F). These results indicate that NHE1 plays a central role in the regulation of ALDH2 by DAPA in cardiomyocytes.

DAPA suppresses the expression of DNMT1 and reduces the promoter methylation level of the ALDH2 gene

To determine the underlying mechanism responsible for the regulation of ALDH2 by DAPA, the changes in the transcription and protein degradation of ALDH2 under DAPA treatment were determined. The mRNA level of ALDH2 was significantly increased whereas the protein degradation of ALDH2 was not altered in the DAPA-treated cardiomyocytes compared with the control cardiomyocytes (Fig. 6A and Supplemental 10 A). Next, we conducted BSP sequencing of the promoter region of ALDH2 and found that ISO increased the promoter methylation level of ALDH2, whereas DAPA reduced ALDH2 promoter methylation (Fig. 6B and C, Supplementary Fig. 10B). Among the DNA methyltransferases, DAPA mainly affected the expression of DNMT1 (Fig. 6D and Supplementary Fig. 10C). Knockdown of DNMT1 increased the expression of ALDH2 in cardiomyocytes

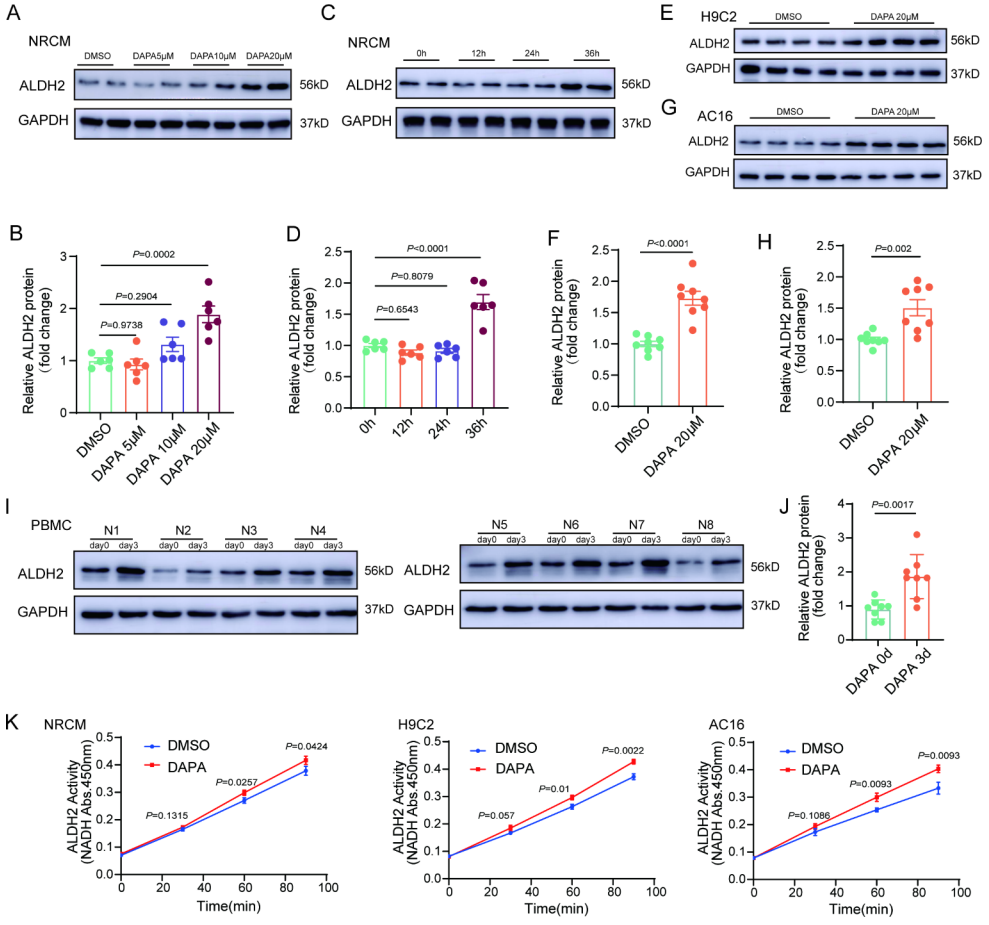

Fig. 4 DAPA can increase the expression and activity of ALDH2 in cardiomyocytes. **A**-**B**, Western blot analysis of ALDH2 levels in neonatal rat cardiomyocytes (NRCMs) treated with different concentrations of DAPA (5, 10, or 20μM, $n=6$). **C**-**D**, Western blot analysis of ALDH2 levels in NRCMs at the indicated time points (12, 24, or 36 h, $n=6$). **E**-**H**, Western blot analysis of ALDH2 levels in AC16 and H9C2 cells treated with DAPA (20μM, 36 h, $n=8$). **I**-**J**, Western blot analysis of ALDH2 levels in peripheral blood mononuclear cells (PBMCs) from patients with type 2 diabetes who took DAPA orally (10 mg, qd) for three days before and after delivery. **K**, ALDH2 activity levels in NRCMs treated with DAPA (20μM, 36 h). *P* values are indicated

(Fig. 6E and F, Supplemental Fig. 10D) and reduced the promoter methylation level of ALDH2 (Fig. 6G).

Next, we investigated the possible molecular mechanism by which DAPA affects DNMT1. SGLT2i can suppress the production of ROS [21] and ROS is an important epigenetic regulator. We hypothesized that ROS may play a key role in the regulation of DNMT1 by DAPA. In cardiomyocytes, DAPA reduced ISO-induced production of ROS (Fig. 6H and I). In TAC-induced hypertrophic hearts, DAPA also decreased the levels of ROS (Fig. 6J and L). Further studies indicated that DNMT1 was increased in H_2O_2-treated cardiomyocytes compared with control cardiomyocytes (Fig. 6M and N).

NAC reduced the levels of ROS in ISO-treated cardiomyocytes (Supplemental Fig. 10E and 10 F). More importantly, NAC decreased the expression of DNMT1 but increased the expression of ALDH2 in ISO-treated cardiomyocytes (Supplemental Fig. 10G and 10 H). These results confirmed that the ROS/DNMT1 pathway plays a critical role in the regulation of ALDH2 by DAPA in cardiomyocytes.

DAPA increases the binding of NFYA to the ALDH2 promoter region

The JASPAR website predicted that NFYA was an important transcription factor for ALDH2 (Fig. 7A). DNMT1 knockdown increased the binding of NFYA to the ALDH2 promoter region (Fig. 7B). Moreover, the binding of NFYA to the ALDH2 promoter region was increased by DAPA (Fig. 7C). Using CUT-Tag, we confirmed that DAPA increased the binding of NFYA but decreased the binding of DNMT1 to the ALDH2 promoter region (Fig. 7D and E).

Histone acetylation plays an important role in modulation gene expression in cardiomyocytes [22]. Then, we detected acetylation-related proteins and found that DAPA did not change the expression of histone acetylation-related enzymes (Supplemental Fig. 11).

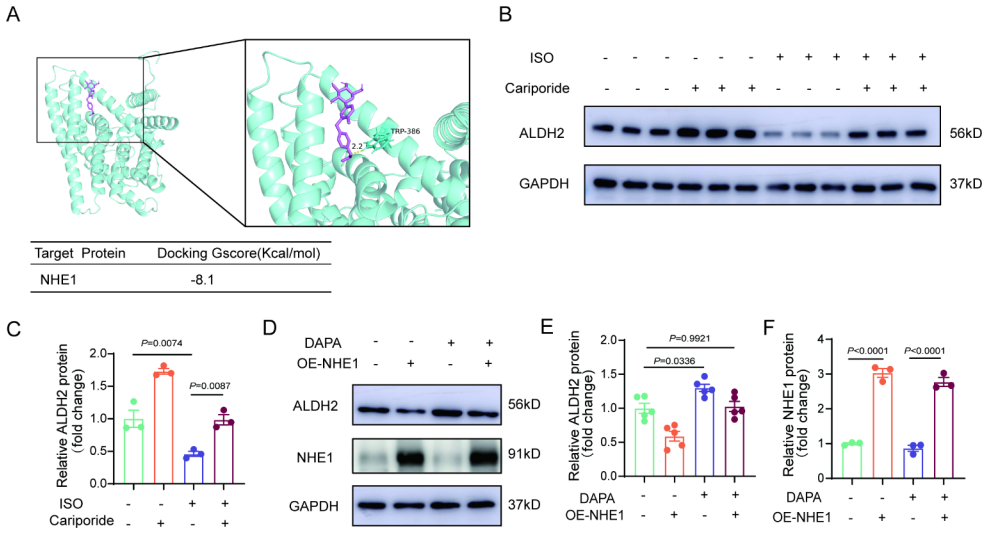

Fig. 5 DAPA targeting NHE1 confers cardioprotective effects. **A**, Molecular docking of DAPA with NHE1. **B**-**C**, Western blot analysis of ALDH2 levels in NRCMs treated with ISO (10μM, 48 h) or Cariporide (10μM, 36 h). **D**-**F**, Western blot analysis of ALDH2 and DNMT1 levels in NRCMs after NHE1 overexpression lentivirus infection). **G**-**H**, Representative immunofluorescence images of intracellular ROS levels after overexpressed-NHE1 cells were treated with DAPA ($n=5$, scale bar = 25 μm). *P* values are indicated

Discussion

Elucidating the underlying molecular mechanism of myocardial remodeling and exploring therapeutic targets reduces the incidence of heart failure [23]. In the present study, we demonstrated that DAPA protects against cardiac remodeling, which could be attributed to increased expression of ALDH2. The application of DAPA reduced the methylation of the ALDH2 promoter region by reducing the levels of ROS and DNMT1, promoted the binding of NFYA to the ALDH2 promoter region, and promoted ALDH2 transcription.

Myocardial remodeling, which is associated with increased interstitial fibrosis, cell death, and contractile dysfunction [24], represents a leading cause of morbidity and mortality worldwide. As this remodeling is associated with the early stage of heart failure, timely intervention is essential [25]. As a first-line hypoglycemic drug, increasing numbers of studies have demonstrated the protective effect of DAPA on cardiovascular disease [26, 27]. These effects include but are not limited to, renal and systemic hemodynamic effects; direct effects on the heart, vasculature, and tubular cells, on- and off-target effects; and numerous other effects [28–30]. Clinical studies have also shown that SGLT2i use is associated with improved quality of life and functional capacity of HF patients [31]. It activated the SIRT1/HIF-1α signaling pathway and had a protective effect on Ang II-induced experimental myocardial hypertrophy in mice [32]. DAPA reduces oxygen radicals and the activity of membrane channels related to calcium transport in ATII-stressed diabetic mice [33]. In our study, we demonstrated that ALDH2 mediates the protective effect of DAPA on myocardial remodeling.

Aldehyde dehydrogenase 2 (ALDH2) is a metabolizing enzyme that detoxifies acetaldehyde and endogenous lipid aldehydes such as 4-hydroxy-2-nonenal (4-HNE) [16]. Numerous clinical and experimental studies have demonstrated the enzymatic and nonenzymatic roles of ALDH2 in cardiovascular disease [34–36]. Most of the previous studies on myocardial remodeling focused on the downstream molecules of ALDH2. Alpha-lipoic acid therapy has been shown to reduce the effects of pressure overload-induced cardiac hypertrophy and remodeling in TAC mice and improve cardiac function through a mechanism dependent on ALDH2 [17]. ALDH2 plays a protective role against diabetic cardiomyopathy by preserving mitochondrial integrity through the Akt-GSK3β pathway and promoting mitophagy via Parkin-dependent mechanisms [37]. However, there is currently a scarcity of drugs or means to target ALDH2 directly. The upstream mechanism of ALDH2 requires further investigation. In our study, we proposed for the first time that DAPA can promote ALDH2 transcription. We employed an innovative approach in which DAPA was used to increase the expression of ALDH2, thereby contributing to the inhibition of cardiac remodeling. Interestingly, our analysis of peripheral blood nucleated cells from patients with type 2 diabetes revealed that DAPA increased ALDH2 expression regardless of genotype.

Many studies have shown that SGLT2 is not expressed in cardiomyocytes and that DAPA has beneficial effects on cardiovascular disease via off-target mechanisms [38–40]. We also confirmed that SGLT2 was not expressed in cardiac cells. As a membrane transporter, NHE-1 regulates the intracellular pH and Na^+ and Ca^{2+} concentrations [41]. NHE-1 hyperactivity is intimately linked to

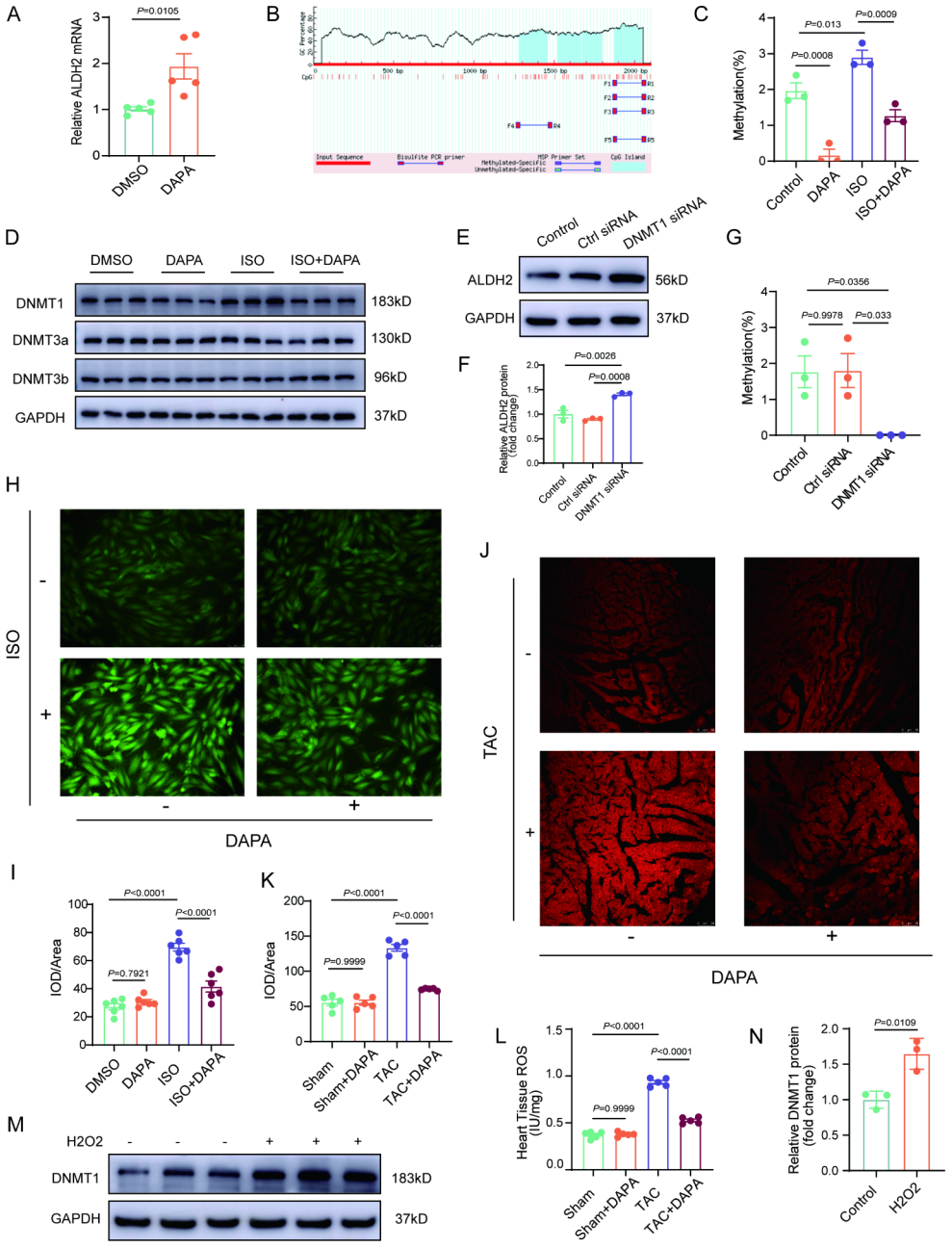

Fig. 6 ROS inhibits ALDH2 expression through DNMT1-mediated methylation. **A**, Real-time quantitative PCR analysis of *ALDH2* mRNA levels in NRCMs treated with DAPA. **B**, Schematic representation of the CpG island of the ALDH2 promoter retrieved from the MethPrimertool. **C**, The percentage of methylated CpGs over total CpGs in the ALDH2 promoter was calculated. **D**, Western blot analysis of DNMTs levels in NRCMs treated with DAPA (20μM, 36 h) and ISO (10μM, 48 h). **E**-**F**, Western blot analysis of ALDH2 levels in NRCMs treated with DNMT1 siRNA. **G**, The percentage of methylated CpGs over total CpGs in the ALDH2 promoter was calculated. **H**-**I**, Representative immunofluorescence images of intracellular ROS levels treated with ISO or DAPA ($n = 6$, scale bar = 25 μm). **J**-**K**, DHE staining of heart tissues from mice treated with TAC or DAPA ($n = 5$, Scale bar = 50 μm). **L**, ROS levels in the heart tissues of the mice were determined by ELISA ($n = 5$). **M**-**N**, Western blot analysis of DNMT1 levels in NRCMs after H2O2 treatment. *P* values are indicated

heart diseases [42]. Recently, it has been reported that empagliflozin can prevent cardiac hypertrophy or heart failure through inhibiting NHE-1 [43, 44]. In our study, we utilized molecular docking prediction to hypothesize that DAPA may provide cardiovascular protection by inhibiting the Na+/H+exchanger (NHE-1).

DAPA can play a cardiovascular protective role by reducing ROS [33, 45, 46]. ROS are critical epigenetic regulators that can increase the expression level of methyltransferases [47]. DNMT1 can be upregulated by the ROS family member, superoxide anion ($O2^{-}$) [48]. DNA methylation at the ALDH2 gene locus is associated with

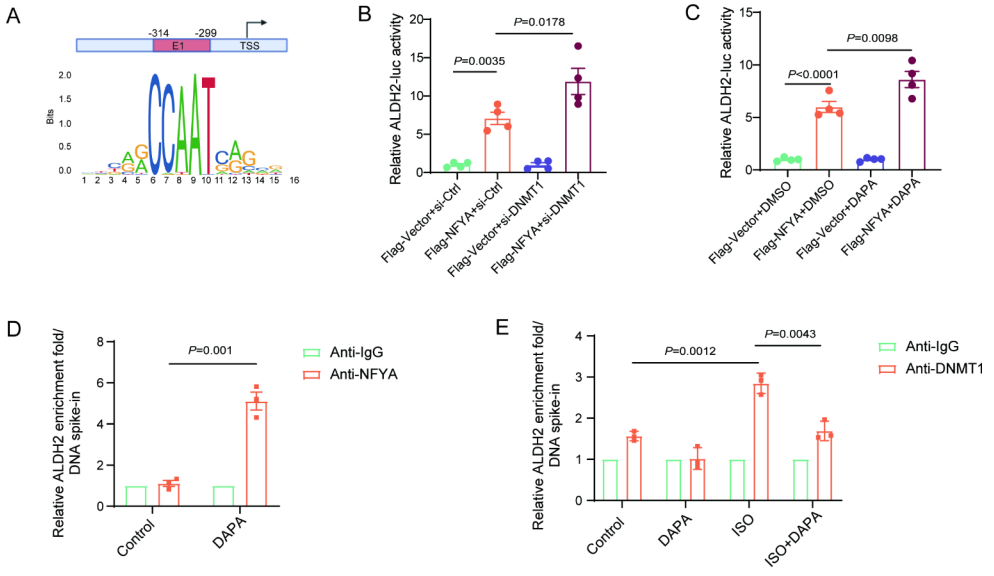

Fig. 7 Inhibition of the key methylation enzyme DNMT1 promotes the binding of NFYA to the ALDH2 promoter region. **A**, Scheme of the predicted NFYA binding sites. **B**, Luciferase assay showing the interplay between NFYA and the ALDH2 promoter in H9C2 cells treated with DNMT1 siRNA. **C**, Luciferase assay showing the interplay between NFYA and the ALDH2 promoter in H9C2 cells treated with DAPA. **D**, H9C2 cells were treated with DAPA. CUT&Tag-qPCR assay of NFYA bound to promoter regions of ALDH2, and ALDH2 gene expression analysis by RT-qPCR. **E**, H9C2 cells were treated with ISO and DAPA. CUT&Tag-qPCR assay of DNMT1 bound to promoter regions of ALDH2, and ALDH2 gene expression analysis by RT-qPCR. *P* values are indicated

the downregulation of ALDH2 expression [49, 50]. Our research revealed that DAPA decreases the methylation level of the ALDH2 promoter region, thereby leading to increased NFYA binding and ultimately resulting in increased ALDH2 expression. In addition to methylation, histone acetylation also plays a vital role in regulating gene expression in cardiomyocytes [22, 51]. Our experiments demonstrated that DAPA cannot change the expression of histone acetylation-related proteins in cardiomyocytes. Thus, DNA methylation but not histone acetylation should mainly contribute to the regulation of ALDH2 expression by DAPA.

In summary, the present study demonstrated that ALDH2 plays a critical role in the protective effect of DAPA on cardiac remodeling. DAPA upregulates ALDH2 through the NHE1/ROS/DNMT1 pathway.

Supplementary Information

The online version contains supplementary material available at https://doi.org/10.1186/s12933-024-02477-8.

Supplementary Material 1

Acknowledgements
None.

Author contributions
Conception and design: Shujian Wei, and Yuguo Chen.Acquisition of data: Han Liu, Bingchen Jiang, Rui Hua, Xuehao Liu, Bao Qiao, and Wenjun WangAnalysis and interpretation of data: Han Liu, and Shujian Wei.Drafting of the article: Shujian Wei.Administrative, technical, or material support: Xiangxin Zhang, Xilong Liu, Qiuhuan Yuan and Bailu Wang.Study supervision: Yuguo Chen.

Funding
This work was supported by the State Key Program of the National Natural Science Foundation of China (82030059), National Natural Science Foundation of China (82072141, 82272240, 82202376), Natural Science Foundation of Shandong Province (ZR2022QH225), and Clinical Research Foundation of Shandong University (2020SDUCRCC014).

Data availability
No datasets were generated or analysed during the current study.

Declarations

Competing interests
The authors declare no competing interests.

Ethical approval
The study adhered to the principles of the Declaration of Helsinki and was approved by the Ethics Committee of Qilu Hospital of Shandong University. All animal studies were approved by the Institutional Animal Care and Use Committee of Qilu Hospital of Shandong University (DWLL-2023-138).

Author details
[1]Department of Emergency and Chest Pain Center, Qilu Hospital of Shandong University, Jinan 250012, Shandong, People's Republic of China
[2]Shandong Provincial Clinical Research Center for Emergency and Critical Care Medicine, Institute of Emergency and Critical Care Medicine of Shandong University, Qilu Hospital of Shandong University, Jinan 250012, Shandong, People's Republic of China
[3]Key Laboratory of Emergency and Critical Care Medicine of Shandong Province, Key Laboratory of Cardiopulmonary-Cerebral Resuscitation Research of Shandong Province, Qilu Hospital of Shandong University, Jinan 250012, Shandong, People's Republic of China
[4]The Key Laboratory of Cardiovascular Remodeling and Function Research, Chinese Ministry of Education, Chinese Ministry of Health and Chinese Academy of Medical Sciences, Qilu Hospital of Shandong University, Jinan 250012, Shandong, People's Republic of China
[5]Department of Intensive Care Unit, Shandong Provincial Hospital Affiliated to Shandong First Medical University, Jinan, Shandong, People's Republic of China

[6]NMPA Key Laboratory for Clinical Research and Evaluation of Innovative Drug, Clinical Trial Center, Qilu Hospital of Shandong University, Jinan 250012, Shandong, People's Republic of China

Received: 27 July 2024 / Accepted: 16 October 2024
Published online: 26 October 2024

References

1. Tani H, Sadahiro T, Yamada Y, Isomi M, Yamakawa H, Fujita R, Abe Y, Akiyama T, Nakano K, Kuze Y, et al. Direct reprogramming improves cardiac function and reverses fibrosis in chronic myocardial infarction. Circulation. 2023;147(3):223–38.
2. Heidenreich PA, Bozkurt B, Aguilar D, Allen LA, Byun JJ, Colvin MM, Deswal A, Drazner MH, Dunlay SM, Evers LR, et al. 2022 AHA/ACC/HFSA Guideline for the management of heart failure: A Report of the American College of Cardiology/American Heart Association Joint Committee on Clinical Practice Guidelines. Circulation. 2022;145(18):e895–1032.
3. Chai R, Xue W, Shi S, Zhou Y, Du Y, Li Y, Song Q, Wu H, Hu Y. Cardiac remodeling in heart failure: role of pyroptosis and its therapeutic implications. Front Cardiovasc Med. 2022;9:870924.
4. Gonzalez A, Ravassa S, Beaumont J, Lopez B, Diez J. New targets to treat the structural remodeling of the myocardium. J Am Coll Cardiol. 2011;58(18):1833–43.
5. Xing J. Venoarterial extracorporeal membrane oxygenation in acute myocardial infarction. Emerg Crit Care Med. 2024;4(1):1–3.
6. McDonagh TA, Metra M, Adamo M, Gardner RS, Baumbach A, Bohm M, Burri H, Butler J, Celutkiene J, Chioncel O, et al. 2021 ESC Guidelines for the diagnosis and treatment of acute and chronic heart failure. Eur Heart J. 2021;42(36):3599–726.
7. Vallon V. The mechanisms and therapeutic potential of SGLT2 inhibitors in diabetes mellitus. Annu Rev Med. 2015;66:255–70.
8. Girerd N, Zannad F. SGLT2 inhibition in heart failure with reduced or preserved ejection fraction: finding the right patients to treat. J Intern Med. 2023;293(5):550–8.
9. Li X, Lu Q, Qiu Y, do Carmo JM, Wang Z, da Silva AA, Mouton A, Omoto ACM, Hall ME, Li J, et al. Direct cardiac actions of the sodium glucose co-transporter 2 inhibitor empagliflozin improve myocardial oxidative phosphorylation and attenuate pressure-overload heart failure. J Am Heart Assoc. 2021;10(6).
10. Ni L, Yuan C, Chen G, Zhang C, Wu X: SGLT2i: beyond the glucose-lowering effect. Cardiovasc Diabetol. 2020;19(1).
11. Santos-Gallego CG, Requena-Ibanez JA, San Antonio R, Ishikawa K, Watanabe S, Picatoste B, Flores E, Garcia-Ropero A, Sanz J, Hajjar RJ, et al. Empagliflozin ameliorates adverse left ventricular remodeling in nondiabetic heart failure by enhancing myocardial energetics. J Am Coll Cardiol. 2019;73(15):1931–44.
12. Maeder MT, Khammy O, dos Remedios C, Kaye DM. Myocardial and systemic iron depletion in heart failure. J Am Coll Cardiol. 2011;58(5):474–80.
13. Angermann CE, Santos-Gallego CG, Requena-Ibanez JA, Sehner S, Zeller T, Gerhardt LMS, Maack C, Sanz J, Frantz S, Fuster V, et al. Empagliflozin effects on iron metabolism as a possible mechanism for improved clinical outcomes in non-diabetic patients with systolic heart failure. Nat Cardiovasc Res. 2023;2(11):1032–43.
14. Chen Y, Peng D. New insights into the molecular mechanisms of SGLT2 inhibitors on ventricular remodeling. Int Immunopharmacol. 2023;118: 110072.
15. Zhao Y, Wang B, Zhang J, He D, Zhang Q, Pan C, Yuan Q, Shi Y, Tang H, Xu F, et al. ALDH2 (Aldehyde Dehydrogenase 2) protects against hypoxia-induced pulmonary hypertension. Arterioscler Thromb Vasc Biol. 2019;39(11):2303–19.
16. Zhang J, Guo Y, Zhao X, Pang J, Pan C, Wang J, Wei S, Yu X, Zhang C, Chen Y, et al. The role of aldehyde dehydrogenase 2 in cardiovascular disease. Nat Rev Cardiol. 2023;20(7):495–509.
17. Li W, Yin L, Sun X, Wu J, Dong Z, Hu K, Sun A, Ge J. Alpha-lipoic acid protects against pressure overload-induced heart failure via ALDH2-dependent Nrf1-FUNDC1 signaling. Cell Death Dis. 2020;11(7):599.
18. Guo H, Yu X, Liu Y, Paik DT, Justesen JM, Chandy M, Jahng JWS, Zhang T, Wu W, Rwere F et al: SGLT2 inhibitor ameliorates endothelial dysfunction associated with the common ALDH2 alcohol flushing variant. Sci Transl Med. 2023;15(680):eabp9952.
19. Rui H, Yu H, Zou D, Chi K, Xu P, Song X, Liu L, Wu X, Wang J, Xue L. Vaspin alleviates pathological cardiac hypertrophy by regulating autophagy-dependent myocardial senescence. Emerg Crit Care Med. 2024;4(1):4–15.
20. Lin K, Yang N, Luo W, Qian J-f, Zhu W-w, Ye S-j, Yuan C-x, Xu D-y, Liang G, Huang W-j, et al. Direct cardio-protection of Dapagliflozin against obesity-related cardiomyopathy via NHE1/MAPK signaling. Acta Pharmacol Sin. 2022;43(10):2624–35.
21. Li X, Wang M, Kalina JO, Preckel B, Hollmann MW, Albrecht M, Zuurbier CJ, Weber NC. Empagliflozin prevents oxidative stress in human coronary artery endothelial cells via the NHE/PKC/NOX axis. Redox Biol. 2024;69: 102979.
22. Costantino S, Paneni F, Mitchell K, Mohammed SA, Hussain S, Gkolfos C, Berrino L, Volpe M, Schwarzwald C, Luscher TF, et al. Hyperglycaemia-induced epigenetic changes drive persistent cardiac dysfunction via the adaptor p66(Shc). Int J Cardiol. 2018;268:179–86.
23. Braunwald E. The war against heart failure: the Lancet lecture. The Lancet. 2015;385(9970):812–24.
24. Catalucci D, Latronico MVG, Ellingsen O, Condorelli G. Physiological myocardial hypertrophy: How and why? FBL. 2008;13(1):312–24.
25. Mudd JO, Kass DA. Tackling heart failure in the twenty-first century. Nature. 2008;451(7181):919–28.
26. Solomon SD, McMurray JJV, Claggett B, de Boer RA, DeMets D, Hernandez AF, Inzucchi SE, Kosiborod MN, Lam CSP, Martinez F, et al. Dapagliflozin in Heart failure with mildly reduced or preserved ejection fraction. N Engl J Med. 2022;387(12):1089–98.
27. Han S, Hagan DL, Taylor JR, Xin L, Meng W, Biller SA, Wetterau JR, Washburn WN, Whaley JM. Dapagliflozin, a selective SGLT2 inhibitor, improves glucose homeostasis in normal and diabetic rats. Diabetes. 2008;57(6):1723–9.
28. Vallon V, Verma S. Effects of SGLT2 inhibitors on kidney and cardiovascular function. Annu Rev Physiol. 2021;83(1):503–28.
29. Chen S, Wang Q, Christodoulou A, Mylonas N, Bakker D, Nederlof R, Hollmann MW, Weber NC, Coronel R, Wakker V, et al. Sodium glucose cotransporter-2 inhibitor empagliflozin reduces infarct size independently of sodium glucose cotransporter-2. Circulation. 2023;147(3):276–9.
30. van der Aart-van der Beek AB, de Boer RA, Heerspink HJL. Kidney and heart failure outcomes associated with SGLT2 inhibitor use. Nat Rev Nephrol. 2022;18(5):294–306.
31. Gao M, Bhatia K, Kapoor A, Badimon J, Pinney SP, Mancini DM, Santos-Gallego CG, Lala A: SGLT2 inhibitors, functional capacity, and quality of life in patients with heart failure. JAMA Network Open. 2024;7(4).
32. Yang J, Li L, Zheng X, Lu Z, Zhou H. Dapagliflozin attenuates myocardial hypertrophy via activating the SIRT1/HIF-1α signaling pathway. Biomed Pharmacother. 2023;165: 115125.
33. Arow M, Waldman M, Yadin D, Nudelman V, Shainberg A, Abraham NG, Freimark D, Kornowski R, Aravot D, Hochhauser E, et al. Sodium-glucose cotransporter 2 inhibitor Dapagliflozin attenuates diabetic cardiomyopathy. Cardiovasc Diabetol. 2020;19(1):7.
34. Yang K, Cui S, Wang J, Xu T, Du H, Yue H, Ye H, Guo J, Zhang J, Li P, et al. Early Progression of abdominal aortic aneurysm is decelerated by improved endothelial barrier function via ALDH2-LIN28B-ELK3 signaling. Adv Sci. 2023;10(32).
35. Zhong S, Li L, Zhang YL, Zhang L, Lu J, Guo S, Liang N, Ge J, Zhu M, Tao Y, et al. Acetaldehyde dehydrogenase 2 interactions with LDLR and AMPK regulate foam cell formation. J Clin Invest. 2019;129(1):252–67.
36. Li W, Yin L, Sun X, Wu J, Dong Z, Hu K, Sun A, Ge J. Alpha-lipoic acid protects against pressure overload-induced heart failure via ALDH2-dependent Nrf1-FUNDC1 signaling. Cell Death Dis. 2020;11(7).
37. Zhang Y, Zou R, Abudureyimu M, Liu Q, Ma J, Xu H, Yu W, Yang J, Jia J, Qian S et al: Mitochondrial aldehyde dehydrogenase rescues against diabetic cardiomyopathy through GSK3β-mediated preservation of mitochondrial integrity and Parkin-mediated mitophagy. J Mol Cell Biol. 2023;15(9).
38. Palmiero G, Cesaro A, Vetrano E, Pafundi PC, Galiero R, Caturano A, Moscarella E, Gragnano F, Salvatore T, Rinaldi L, et al. Impact of SGLT2 inhibitors on heart failure: from pathophysiology to clinical effects. Int J Mol Sci. 2021;22(11).
39. Uthman L, Baartscheer A, Schumacher CA, Fiolet JWT, Kuschma MC, Hollmann MW, Coronel R, Weber NC, Zuurbier CJ. Direct cardiac actions of sodium glucose cotransporter 2 inhibitors target pathogenic mechanisms underlying heart failure in diabetic patients. Front Physiol. 2018;9:1575.
40. Berger JH, Matsuura TR, Bowman CE, Taing R, Patel J, Lai L, Leone TC, Reagan JD, Haldar SM, Arany Z, et al. SGLT2 inhibitors act independently of SGLT2 to confer benefit for HFrEF in mice. Circ Res. 2024.
41. Xia H, Zahra A, Jia M, Wang Q, Wang Y, Campbell SL, Wu J. Na(+)/H(+) Exchanger 1, a potential therapeutic drug target for cardiac hypertrophy and heart failure. Pharmaceuticals. 2022;15(7).
42. Yeves AM, Ennis IL. Na(+)/H(+) exchanger and cardiac hypertrophy. Hipertens Riesgo Vasc. 2020;37(1):22–32.

43. Chen S, Overberg K, Ghouse Z, Hollmann MW, Weber NC, Coronel R, Zuurbier CJ. Empagliflozin mitigates cardiac hypertrophy through cardiac RSK/NHE-1 inhibition. Biomed Pharmacother. 2024;174: 116477.
44. Chen S, Wang Q, Bakker D, Hu X, Zhang L, van der Made I, Tebbens AM, Kovacshazi C, Giricz Z, Brenner GB, et al: Empagliflozin prevents heart failure through inhibition of the NHE1-NO pathway, independent of SGLT2. Basic Res Cardiol. 2024.
45. Chang W-T, Shih J-Y, Lin Y-W, Chen Z-C, Kan W-C, Lin T-H, Hong C-S. Dapagliflozin protects against doxorubicin-induced cardiotoxicity by restoring STAT3. Arch Toxicol. 2022;96(7):2021–32.
46. Santos-Gallego CG, Requena-Ibáñez JA, Picatoste B, Fardman B, Ishikawa K, Mazurek R, Pieper M, Sartori S, Rodriguez-Capitán J, Fuster V, et al. Cardioprotective effect of empagliflozin and circulating ketone bodies during acute myocardial infarction. Circ Cardiovasc Imaging. 2023;16(4).
47. Zhao Y, Fan X, Wang Q, Zhen J, Li X, Zhou P, Lang Y, Sheng Q, Zhang T, Huang T, et al. ROS promote hyper-methylation of NDRG2 promoters in a DNMTS-dependent manner: contributes to the progression of renal fibrosis. Redox Biol. 2023;62: 102674.
48. Campos AC, Molognoni F, Melo FH, Galdieri LC, Carneiro CR, D'Almeida V, Correa M, Jasiulionis MG. Oxidative stress modulates DNA methylation during melanocyte anchorage blockade associated with malignant transformation. Neoplasia. 2007;9(12):1111–21.
49. Yang M, Wang A, Li C, Sun J, Yi G, Cheng H, Liu X, Wang Z, Zhou Y, Yao G, et al. Methylation-induced silencing of ALDH2 facilitates lung adenocarcinoma bone metastasis by activating the MAPK pathway. Front Oncol. 2020;10.
50. Tran T-O, Vo TH, Lam LHT, Le NQK. ALDH2 as a potential stem cell-related biomarker in lung adenocarcinoma: Comprehensive multi-omics analysis. Comput Struct Biotechnol J. 2023;21:1921–9.
51. Costantino S, Camici GG, Mohammed SA, Volpe M, Lüscher TF, Paneni F. Epigenetics and cardiovascular regenerative medicine in the elderly. Int J Cardiol. 2018;250:207–14.

Publisher's note